JOC The Journal of Organic Chemistry

Featured Article

pubs.acs.org/joc

3-(Dialkoxyphosphoryl)-N-confused Phlorin and Porphyrin. Synthesis, Stereochemistry, and Coordination Properties

Bin Liu,[†] Xiaofang Li,*[,†] Xin Xu,[†] Marcin Stępień,[‡] and Piotr J. Chmielewski*[,‡]

[†]Key Laboratory of Theoretical Chemistry and Molecular Simulation of Ministry of Education, Hunan Province College Key Laboratory of QSAR/QSPR, School of Chemistry and Chemical Engineering, Hunan University of Science and Technology, Xiangtan, Hunan 411201, China

[‡]Department of Chemistry, University of Wrocław, 14 F. Joliot-Curie Street, 50 383 Wrocław, Poland

Supporting Information

ABSTRACT: A 3-phosphonated N-confused phlorin **3** was synthesized by the reaction of N-confused porphyrin **1** and trimethyl or triethyl phosphite **2** in the presence of acetic acid in good yield. The presence of hydrogen and aryl substituents in one of the *meso* positions (C5) generates a stereogenic center, resulting in configurationally stable enantiomers. The enantiomers were separated by HPLC and characterized by the circular dichroism method for the first time in the case of phlorin. Further oxidation of **3** by DDQ (2,3-dichloro-5,6-dicyano-1,4-benzoquinone) afforded the achiral 3-phosphonated N-confused porphyrin **4**. Chiral chlorozinc **4**−Zn and chlorocadmium **4**−Cd, as well as achiral nickel(II) complexes **4**−Ni were also characterized. For **4**−Cd in the solid state, formation of a dimer consisting of heterochiral subunits joined by two H-bonds was established by a single crystal X-ray analysis. For **4**−Cd, separation of enantiomers was achieved. Slow racemization of **4**−Cd in solution prevented the absolute configuration determination by the X-ray method indicating the labile character of the complex. The relationship between circular dichroism and absolute configuration of **3a** and **4**−Cd was established on the basis of TD-DFT calculations.

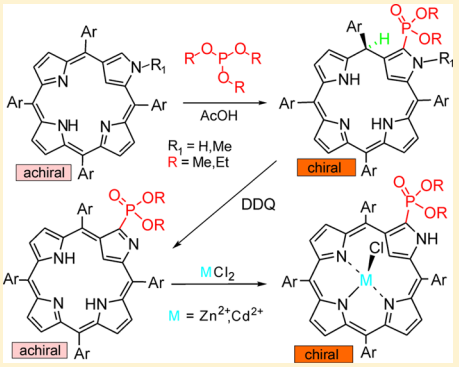

INTRODUCTION

2-Aza-21-carbaporphyrins (N-confused porphyrins, NCP, **1**), porphyrin isomers containing a pyrrole moiety incorporated to the macrocyclic ring by *meso*-α and *meso*-β linkages, have attracted considerable attention in recent years[1−3] because of their potential applications in catalysis[4,5] and molecular sensing[6−8] as well as in supramolecular,[9−12] materials,[11,13,14] and medical chemistry.[15−18] Chemical modification of the macrocycle and coordination chemistry are the two main directions in current research on NCPs. With some exceptions, the modifications focus on the *confused* pyrrole which has three main reaction sites, i.e., N2 (external nitrogen),[19−23] C3 (external carbon),[23−27] and C21 (internal carbon).[28−35] The reactivity of the C3−N2 bond on the periphery of NCP, which is partially isolated from the macrocyclic conjugation pathway, resembles that of a C═N fragment in some aza-aromatic systems (quinolines, isoquinolines). Previously, we have shown that in the case of NCP such reactivity results in a regiospecific substitution at C3 by cyclic substrates containing active methylene.[25] Formation of phlorin-type products involving N2 and *meso*-position C20 as targets for the 1,3-dipolar agents is also a consequence of that kind of reactivity.[36] Inspired by the known reactivity of pyridines or isoquinolines toward trialkyl phosphites,[37−39] which offers a convenient route to phosphorylated derivatives, we have decided to apply a similar protocol in the phosphorylation of NCP. Introduction of phosphorus-bearing substituents to the position C3 and/or C21 by the reaction of NCP or its trivalent silver complex with potassium diphenylphosphide has been recently reported,[40] following the observation of similar reactivity of carbaporpholactone.[41] A related catalytic dialkoxyphosphorylation of β-carbons in a reaction of diethyl phosphite with bromoporphyrins has been very recently reported for regular porphyrins,[42] indicating a considerable interest in the phosphorylated porphyrin systems. Porphyrins with phosphine or phosphonate substituents at one or two *meso* positions have been shown to form oligomers or networks in which metalloporphyrin subunits are linked by P- or O-coordination to the metal ion.[43] Thus, introduction of such substituents allows not only for fine alteration of the coordination properties of the macrocyclic interior but also provides an additional donor group on the perimeter.[44−47]

In our search for new and potentially useful optically active and configurationally stable systems, we focus on the nonplanar derivatives of NCP and their complexes which are intrinsically chiral.[48] In this paper, we present for the first time the resolution of the enantiomers of a chiral phlorin and of a chiral complex of a Group 12 metal of the NCP derivative.

RESULTS AND DISCUSSION

NCP (**1**) was reacted with trimethyl or triethyl phosphite in the presence of acetic acid in refluxing anhydrous benzene to produce the desired product **3** in moderate to good yields (Scheme 1). The reaction also proceeded at room temperature, though under such conditions a higher molar excess of the

Received: December 10, 2012
Published: January 23, 2013

   dx.doi.org/10.1021/jo302689d | J. Org. Chem. 2013, 78, 1354−1364

Scheme 1. Synthesis of 3-Phosphorylated N-Confused Phlorins

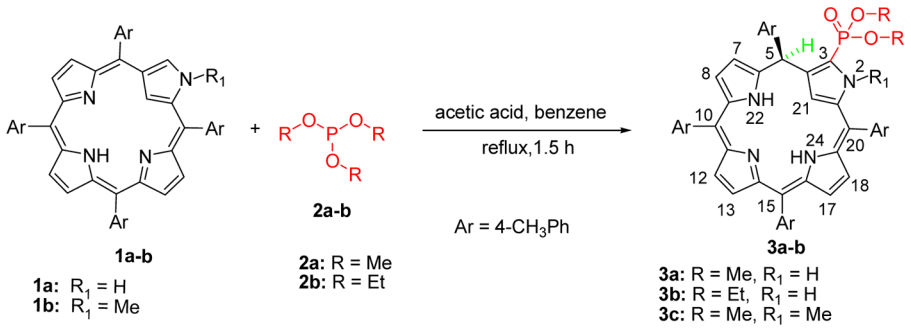

phosphite **2** was required (about 20-fold). The color of the solution gradually changed from brown-green to blue-green. The progress of the reaction was monitored by TLC, and the target products were purified by flash column chromatography on silica gel and identified as the 3-phosphorylated N-confused phlorin **3** on the basis of its mass, UV−vis, and NMR (^{1}H, ^{13}C, ^{31}P, COSY, HSQC, HMBC, NOESY) spectra.

The mass spectrum (MALDI-TOFMS) of **3a** revealed the molecular ion peak at m/z 781, consistent with the addition of a dimethoxyphosphoryl group to NCP. The UV−vis spectrum of **3** (Figure 1), characterized by two major bands at ∼415 and

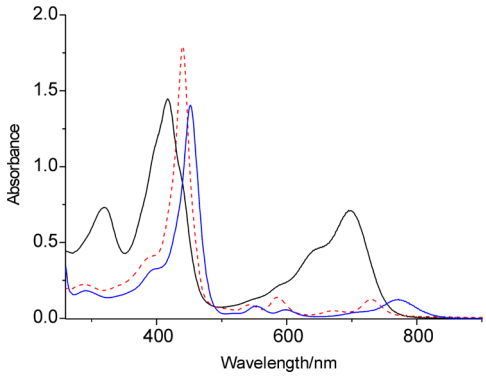

Figure 1. UV−vis spectra of phlorin **3b** (black solid line) and porphyrin **4b** (blue solid line), and starting porphyrin **1a** (red dotted line) in dichloromethane.

696 nm, resembles those observed for N-confused phlorins,[36] S-confused phlorin,[49] or regular phlorins[50−52] and considerably differs from the spectrum of the starting NCP.

The ^{1}H NMR spectrum of **3a** is shown in Figure 2A along with the partial signal assignments. The ^{1}H NMR spectrum of **3a** in $CDCl_3$ is characterized by six β-pyrrole proton signals in the region of 6.55−6.96 ppm; thus, they are all shifted upfield with respect to those in the spectrum of NCP (**1a**) in the same solvent. The inner 21-CH signal of the *confused* pyrrole appearing in the spectrum of **1a** at about −5 ppm is remarkably shifted downfield to δ_H 5.37 ppm in the spectrum of **3a**. In the spectrum of **3a** this signal appears as a doublet of doublets due to scalar couplings with (a) 2-NH resonating at δ_H 9.05 ppm ($^4J_{HH}$ = 2.4 Hz) and (b) the phosphorus bound in the position 3 ($^4J_{HP}$ = 4.4 Hz). The inner 22,24-NH proton signals of porphyrin **1a** resonate around δ_H −2.5 ppm at low temperatures, whereas in the phlorin **3a** appear in a region of 8.2−8.8 ppm. The assignment of the NH signals was confirmed by deuterium exchange experiments with D_2O. Three singlets at δ_H 2.22, 2.41, and 2.43 ppm are assigned to four methyls of meso *p*-tolyl substituents. Two doublets at δ_H 3.38 and 3.81 ppm with coupling constants $^3J_{HP}$ = 11.5 Hz are those of methoxyls on the phosphoryl fragment. The upfield shift of the pyrrole signals and the downfield shift of the 21-CH, 22-NH, and 24-NH peaks indicate the absence of a macrocyclic aromatic ring current in **3a**. In the ^{13}C NMR spectrum of **3a**, two doublets at δ_C 52.9 and 53.1 ppm ($^2J_{CP}$ = 4.7 and 3.9 Hz, respectively) were assigned on the basis of heteronuclear 2D experiments to the methoxyl carbons of the phosphonate group and the singlet at δ_C 41.7 ppm was assigned to the meso position C5, whereas the doublet at δ_C 104.8 ppm ($^4J_{CP}$ = 13.2 Hz) was assigned to the internal carbon C21. The ^{13}C−^{1}H HMBC spectrum allowed an assignment of the C3 signal which is a doublet centered at δ_C 112.7 ppm ($^1J_{CP}$ = 225.2 Hz). The signal at δ_P 13.9 in the ^{31}P{^{1}H} NMR spectrum of **3a** indicated the presence of a phosphonate group, while the ^{31}P−^{1}H HMBC experiment confirmed scalar couplings of phosphorus with neighboring protons.

A low-temperature ^{1}H−^{1}H COSY spectrum (235 K, $CDCl_3$) confirmed scalar couplings between the "inner" and "outer" protons. Two NH protons that are located within the macrocyclic ring and resonate at δ_H 8.23 and 8.75 ppm correlate with two pairs of β-pyrrole protons resonating at δ_H 6.82, 7.03 ppm and at δ_H 6.68, 6.71 ppm, respectively. The 2-NH located on the *confused* pyrrole whose signal appears at δ_H 9.06 ppm correlates with 21-CH at δ_H 5.29 ppm. From the low-temperature ^{1}H−^{1}H NOESY experiment (235 K, $CDCl_3$) indicating through-space interaction between 21-CH and 22,24-NH their common intra-annular location can be inferred. In addition, correlations of 5-CH with methoxy protons of the phosphonate group observed in the NOESY map were vital for the signal assignment and structure elucidation. Similar spectroscopic characteristics are displayed by the 3-diethylphosphonated phlorin **3b** and the 2-methylated derivative **3c**, with obvious differences related to the different substituent patterns.

NMR spectroscopy provides strong evidence for the nonplanarity of the macrocycle and its consequent chirality. It is reflected in the first instance by the number of alkoxyl signals of the phosphoryl group. The faces of the macrocycle are nonequivalent, and thus, the methoxy signals are differentiated in the spectra of **3a** and **3c**, while for the diethoxyphosphonated derivative **3b** the methylene signals of two magnetically inequivalent ethoxy groups are diastereotopic. These spectral features unequivocally indicate chirality of the phlorin systems.

The single-crystal X-ray diffraction analysis performed for **3b** confirms that the structural features derived from the solution studies are also present in the solid state (Figure 3). Locations of the phosphoryl group on C3 and the pyramidal carbon in the *meso*-position 5 are apparent. The nonconfused pyrrole moieties are essentially planar, and their structures are similar to those observed in regular phlorins.[51] Except for the C5 center, each of the meso bridges is nearly coplanar with two adjacent pyrrole rings. Nitrogen-bound hydrogens were identified in the difference

dx.doi.org/10.1021/jo302689d | J. Org. Chem. 2013, 78, 1354−1364

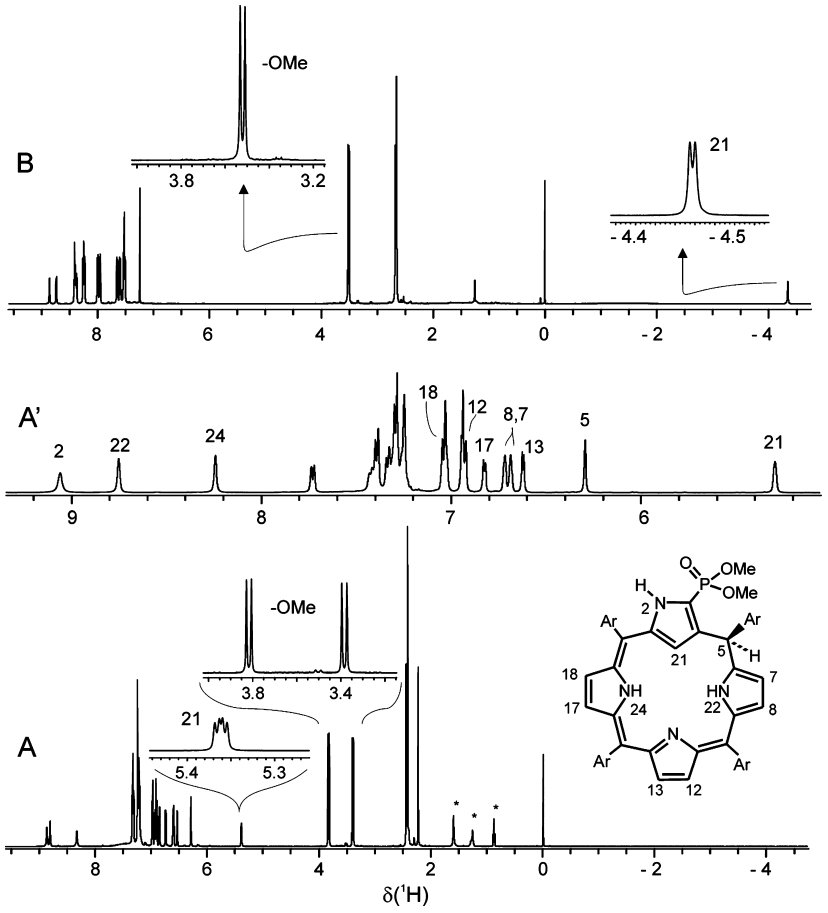

Figure 2. ^{1}H NMR spectrum (500 MHz, $CDCl_3$) of **3a** at 300 K (A), low-field part of the spectrum of **3a** recorded at 235 K with a partial signal assignment (A′), and ^{1}H NMR spectrum (500 MHz, 300 K, $CDCl_3$) of **4a** (B). Expansions of indicated signals are shown in the insets.

density map at positions N2, N22, and N24. Due to the presence of a stereogenic center at C5, the molecule is chiral. Nevertheless, compound **3b** crystallizes as a racemic phase in the centrosymmetric $P\bar{1}$ space group, and thus the crystallographic unit cell consists of a pair of symmetry-related enantiomers. Analysis of the nonbonding distances in the crystal lattice reveals the occurrence of intermolecular CH/π H-bonds[53] between the unique *p*-tolyl substituent at C5 and the π-conjugated system of the neighboring molecule, mainly the pyrrole subunit comprising the N22 atom and the *confused* pyrrole (Figure 4). Owing to that interaction, the crystal lattice is organized into homochiral columns for both enantiomers.

Separation of the enantiomers of **3b** was achieved by means of HPLC on the chiral stationary phase. It resulted in an enantiomerically pure fraction containing the faster migrating enantiomer, while in the second fraction, the enantiomeric excess of the slower migrating isomer was 90% because of a partial overlap of the chromatographic bands (Figures 5A–C). The circular dichroism spectra of these fractions are almost perfect mirror images to each other, and both reveal two Cotton effects of opposite signs at the wavelengths of the major bands of the optical spectrum of **3b** (Figure 5). The CD spectrum reflects the intrinsic chirality of the phlorin ring, whose optical activity is extended on the whole chromophore. To the best of our knowledge, this is the first example of an optically active phlorin. To correlate the chirooptical response of the enantiomers with their absolute configuration we calculated the electronic transitions for the *R* enantiomer of phlorin **3b** by means of the time-dependent density functional theory (TD-DFT). The calculated CD spectrum pattern is in very good agreement with that recorded for the faster-migrating enantiomer **1** allowing the assignment of its configuration as *R*.

The reaction path leading from NCP to the phosphorylated phlorin **3** (Scheme 2) involves activation of the porphyrin by an acid, a step that was observed previously in several instances of the reaction occurring at C3.[24,25] In the case of NCP (**1a**), the most likely activation process is protonation of the N2 position, whereas for **1b**, a similarly activated form can be obtained by internal protonation of the macrocycle. Apparently, that additional NH, once attached, stays with the macrocycle until formation of the final phlorin **3** is completed, and unlike in the cases of previously reported acid-catalyzed reactions,[24,25] it is not efficiently abstracted by atmospheric oxygen even when no effort has been made to eliminate autoxidation. Instead of dehydrogenation, an H-shift from C3 to C5 is operative upon attachment of the phosphorus nucleophile. The acetate anion takes an important part in the reaction mechanism as a dealkylating agent, converting the cationic tris(alkoxy) moiety into a neutral dialkoxyposphoryl group. That was verified by means of the ^{1}H NMR-monitored reaction carried out for the **1a**/$P(OEt)_3$/AcOH system in C_6D_6 where formation of the equivalent amount of ethyl acetate was observed concurrently with the formation of **3b**.

Although the phlorins **3** are relatively stable toward autoxidation and their solutions can be handled in the presence of daylight and air, they are slowly converted into other products by atmospheric oxygen. One of these products can be efficiently obtained by the reaction of **3** with a strong oxidant, e.g., 2,3-dichloro-5,6-dicyano-1,4-benzoquinone (DDQ), followed by chromatographic workup

dx.doi.org/10.1021/jo302689d | *J. Org. Chem.* 2013, 78, 1354–1364

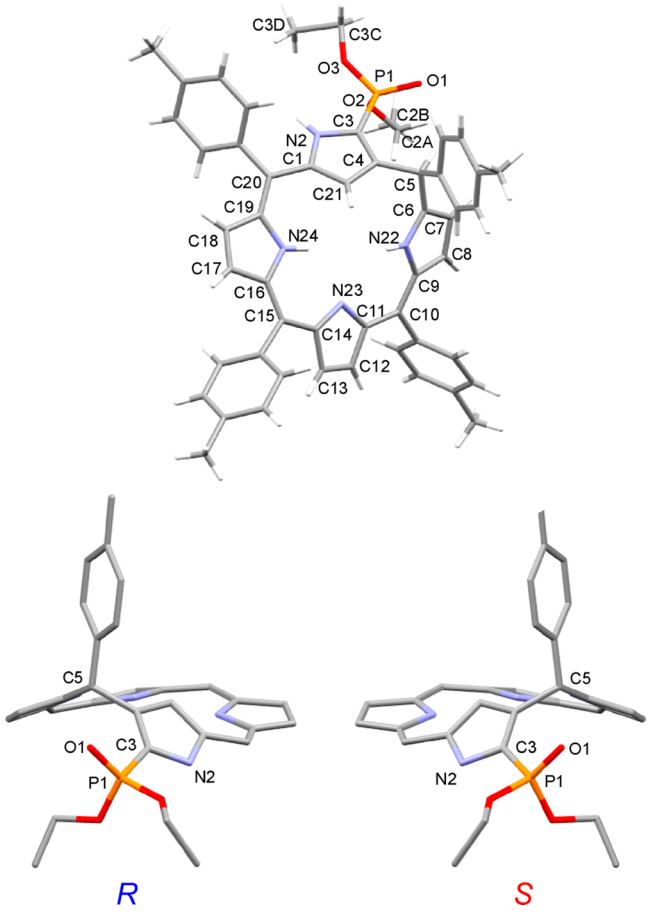

Figure 3. Perspective view and atom numbering of the molecular structure of **3b** (*R* enantiomer, top). The cocrystallized chloroform solvent molecule is omitted. In the bottom, the side views of both enantiomers are presented. All hydrogen atoms and aryl substituents except for that at C5 are omitted for clarity.

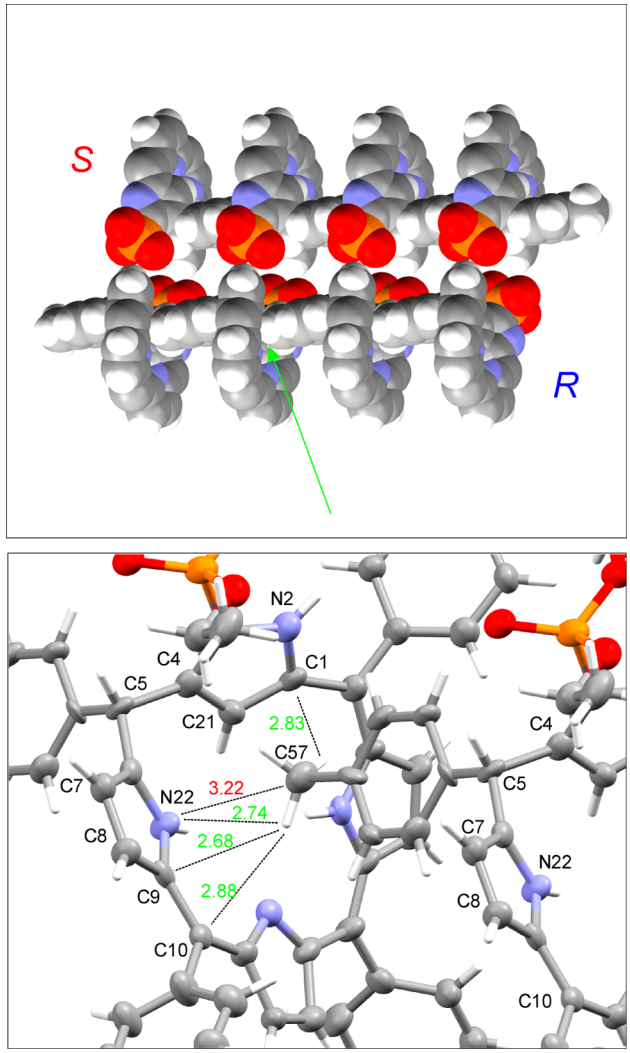

Figure 4. Lower box: Partial packing diagram for the crystal structure of **3b** (30% probability ellipsoids) showing interatomic contacts between overlapping parts of neighboring molecules. The nonbonding distances (in Å) between non-hydrogen atoms and hydrogens at C57 (placed in the idealized positions) are presented as green numbers. Upper box: A space-filling representation of a fragment of the crystal lattice of **3b** showing spatial arrangement of enantiomeric columns. The green arrow indicates a site of C57. Solvent molecules, ethyl substituents, and aryls in the positions 10, 15, and 20 are omitted for clarity.

(Scheme 3). The product **4** was identified as 3-(dialkoxyphosphoryl)-N-confused porphyrin, and it is apparently formed by dehydrogenation of the positions 2 and 5 of the phlorin **3**. Such reactivity is rare among isolable phlorins[49] because they usually comprise a tetrahedral carbon with two non-hydrogen substituents in the *meso*-position and their conversion into an aromatic macrocycle such as porphyrin or chlorin is prevented.

The structures of the 3-phosphorylated NCP's were confirmed by high-resolution mass spectrometry, UV−vis, and multinuclear NMR. In the ESI-MS spectra the molecular ion peaks at m/z 779.3145 (calcd 779.3146 for $[M + H]^+$) for **4a** and at 807.3444 (calcd 807.3459 for $[M + H]^+$) for **4b** indicate abstraction of two hydrogen atoms from **3a** or **3b**, respectively. The UV−vis spectra of **4a** or **4b** are characterized by six major bands at 290, 395, 452, 554, 600, and 770 nm. Their spectral pattern resembles that of the starting porphyrin **1a**, although all these bands are significantly red-shifted in **4**; the Soret band is shifted by 11 nm, and for the Q-band appearing at the longest wavelength the red shift is about 40 nm (Figure 1). The ^{1}H NMR spectra indicate an aromatic character of the macrocycles consisting of 21-CH signal at δ_H −4.33 ppm ($^4J_{HP}$ = 2.3 Hz), a broad signal of the inner NHs at δ −1.5 ppm, and signals of the β-pyrrole protons in the region of 8.3−8.9 ppm. A doublet at δ_H 3.52 ppm ($^3J_{HP}$ = 11.0 Hz) in the spectrum of **4a** is that of the methoxy protons of the dimethylphosphonate group, which are magnetically equivalent, unlike in the case of the nonplanar phlorin **3a**. Likewise, the methyl protons of the ethoxy groups in the spectrum of **4b** give rise to a single triplet at δ_H 1.00 ppm. The methylene protons of the ethoxy groups are diastereotopic, and two multiplets appear at δ_H 3.84 and 3.94 ppm. ^{1}H−^{31}P HMBC experiments reveal that 21-CH as well as methylene and methyl protons of the substituents at the phosphoryl fragment are scalar coupled to the phosphorus resonating at δ_P 11.6 ppm.

To check whether the phosphoryl group at the position 3 can alter the properties of the NCP coordination core we attempted the insertion of nickel(II), zinc, and cadmium into **4** (Scheme 4).

In the case of nickel(II), the spectroscopic characteristics indicate the formation of a square planar, diamagnetic species (**4**−Ni) whose ^{1}H NMR spectral pattern differs from that of the unsubstituted NCP−nickel(II) complex by the absence of the 3-CH signal and the presence of the ethoxyl signals (300 K, CD_2Cl_2).[2] Methyl and methylene protons each give one signal at δ_H 1.19 and 3.87 ppm, respectively indicating magnetic equivalency of both

dx.doi.org/10.1021/jo302689d | J. Org. Chem. 2013, 78, 1354−1364

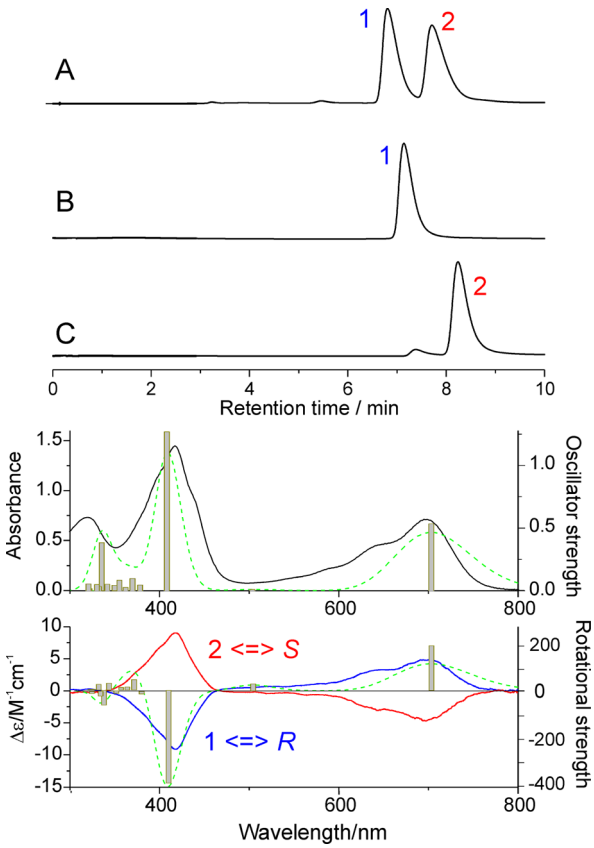

Figure 5. Top: Chiral-phase HPLC profiles (0.5 mg of solute, eluent dichloromethane, flow 1 mL/min, detection at λ = 520 nm) of the racemic **3b** (A) and separated fractions 1 (B) and 2 (C). Bottom: UV–vis and CD spectra of the separated fractions (dichloromethane solutions). The gray bars represent electronic transitions calculated for the *R* enantiomer (PCM-TD-B3LYP/6-311G**//6-31G**). The spectra calculated for the enantiomer *R* are traced as green dashed lines.

ethoxyls and, consequently, an effective planarity of the system. The methylene signal is split into doublet of quartets with $^{2}J_{HP}$ = 7.8 Hz and $^{3}J_{HH}$ = 7.1 Hz. Otherwise, the spectral features are indicative of the coordination mode typical of NCP–nickel(II) complexes,[2] and those include the presence of a proton on the outer nitrogen N2 resonating at δ_H 10.61 ppm and a lack of any protons inside the macrocyclic core as well as reduction of the aromaticity with respect to that of the free base. Ethoxyl protons (both methylenes and methyls) and 2-NH correlate in the $^{1}H-^{31}P$ HMBC with phosphorus resonating at δ_P 6.9 ppm. The presence of the nickel ion can be derived from the HRMS (ESI-TOF) giving a molecular ion peak at 863.2656 (calcd 863.2656 for $[M + H]^+$). In the UV–vis absorption spectrum of **4**–Ni (Figure 6), the Soret region (250–450 nm) resembles those of the unsubstituted or 2-alkylated NCP nickel(II) complexes.[2] However, Q-bands appearing at the longest wavelengths are considerably red-shifted (50–80 nm) in **4**–Ni.

Zinc(II) and cadmium(II) derivatives of **4** were obtained under very mild conditions by stirring the ligand with an excess of the corresponding anhydrous metal chloride in dichloromethane (Scheme 4) followed by separation of the complex from the inorganic salt by washing with water (in the case of **4**–Zn) or filtration and crystallization (**4**–Cd). ESI mass spectra confirm coordination of metals by the presence of fragmentation peaks at *m*/*z* 841.2272 (841.2281 calcd $[M - Cl]^+$ for **4**–Zn) and at *m*/*z* 919.2361 (919.2350 calcd $[M - Cl]^+$ for **4**–Cd) and, in the case of **4**–Cd, also by molecular ion peak at *m*/*z* = 955.2100 (955.2110 calcd for $[M + H]^+$), which indicates the presence of a chloride ligand. Spectral characteristics of both complexes are indicative of the coordination mode typical for adducts of the Group 12 metals with NCP acting as a monoanion. Those include proton signals of 2-NH (δ_H 9.08 ppm for **4**–Zn and 9.38 ppm for **4**–Cd) and 21-CH (δ_H 1.24 ppm for **4**–Zn and 1.24 ppm for **4**–Cd) appearing in the low- and high-field parts of their ^{1}H NMR spectra, respectively, and lack of the "internal" NH's. These protons are scalar coupled to each other as it can be inferred from the COSY experiments. The position of the 21-CH for **4**–Zn is considerably shifted downfield ($\Delta\delta$ = 2–5 ppm) with respect to those observed in the spectra of monomeric[54] or dimeric[54,55] zinc complexes of NCP, which may be attributed to the presence of the electron-withdrawing dialkylphosphoryl substituent in position 3 of the *confused* pyrrole. A scalar interaction of 21-CH with the ^{31}P nucleus resonating at δ_P 8.9 and 5.4 ppm in the case of **4**–Zn and **4**–Cd, respectively, can be deduced from the $^{1}H-^{31}P$ HMBC spectra for both complexes. These interactions yield $^{4}J_{HP}$ coupling constants of 4.1 Hz for **4**–Zn and 3.9 for **4**–Zn. The scalar coupling to ^{31}P is also observed in the ^{13}C NMR spectra for the C21 resonance (δ_C 72.5 ppm, $^{3}J_{CP}$ = 11.5 Hz for **4**–Zn; δ_C 69.6 ppm, $^{3}J_{CP}$ = 10.5 Hz for **4**–Cd). The doublet corresponding to the C3 center, which is directly bound to the phosphorus atom can be identified on the basis of $^{1}H-^{13}C$ HMBC experiment at δ_C 107.1 ppm ($^{1}J_{CP}$ = 218 Hz) and at δ_C 110.0 ppm ($^{1}J_{CP}$ = 204 Hz) for the zinc and cadmium derivatives, respectively. In each of the complexes, the macrocycle is nonplanar and its two faces are nonequivalent. Consequently, the molecules of **4**–Zn and **4**–Cd are chiral, which results in differentiation of ^{1}H and ^{13}C signals of alkyls attached to the phosphoryl group. Thus, there are two doublets of phosphonate methyls in the ^{1}H NMR spectrum of **4**–Zn at δ_H = 3.11 ppm ($^{3}J_{HP}$ = 12.0 Hz) and 3.35 ppm ($^{3}J_{HP}$ = 11.5 Hz) and at δ_C = 53.0 ppm ($^{2}J_{CP}$ = 6.1 Hz) and 54.2 ppm ($^{2}J_{CP}$ = 4.2 Hz) in the ^{13}C NMR spectrum of this complex. In addition, methyls of the ethoxy-subsituents in **4**–Cd are magnetically inequivalent, giving two triplets, while the two diasterotopic methylene fragments appear in the ^{1}H NMR as four multiplets and in ^{13}C NMR spectrum give two doublets at δ_C = 62.8 ppm ($^{2}J_{CP}$ = 5.3 Hz) and 64.0 ppm ($^{2}J_{CP}$ = 4.0 Hz). In the case of **4**–Cd, a spin–spin coupling with $^{111,113}Cd$ allows observation of "cadmium satellites" associated with signals of certain protons in the ^{1}H NMR spectrum (Figure 7). For all β-pyrrole protons, the coupling constants $^{4}J_{HCd} \sim 3.6–4.9$ Hz confirm the coordination of the "regular" part of the porphyrin,[56] while in the case of 21-CH, the observed value of J_{HCd} is 11 Hz. This value is close to that reported for dimeric cadmium complexes of NCP (12 Hz)[55] but it is considerably higher than that observed for other systems consisting of side-on η^1 or η^2 coordinated aromatic CH such as cadmium complexes of benziporphyrins (7.5 Hz for *m*- and 4.4 Hz for *p*-benziporphyrin).[57,58]

Single-crystal X-ray diffraction analysis of **4**–Cd (Figure 8) unequivocally confirmed the structure of the complex, indicating the presence of cadmium inside the macrocycle, coordination of the "internal" nitrogens (distances Cd1–N(22–24): 2.267(4), 2.221(4), 2.258(4) Å), and an apical chloride (distance Cd1–Cl1 2.3995(16) Å) as well as a weak interaction of a side-on π-bonding type between metal and C21 (distance Cd1–C21 2.579(5) Å). All these distances are shorter than those reported for the analogous complex of S-confused porphyrin.[49] The *confused* pyrrole is considerably tipped out of the mean porphyrin plane P_{21} defined by 21 heavy atoms of the macrocyclic ring (i.e., all except for N2, C3, and C21). A dihedral angle between the mean plane of the

dx.doi.org/10.1021/jo302689d | J. Org. Chem. 2013, 78, 1354–1364

Scheme 2. Proposed Mechanism of the Formation of 3-Phosphorylated Phlorins

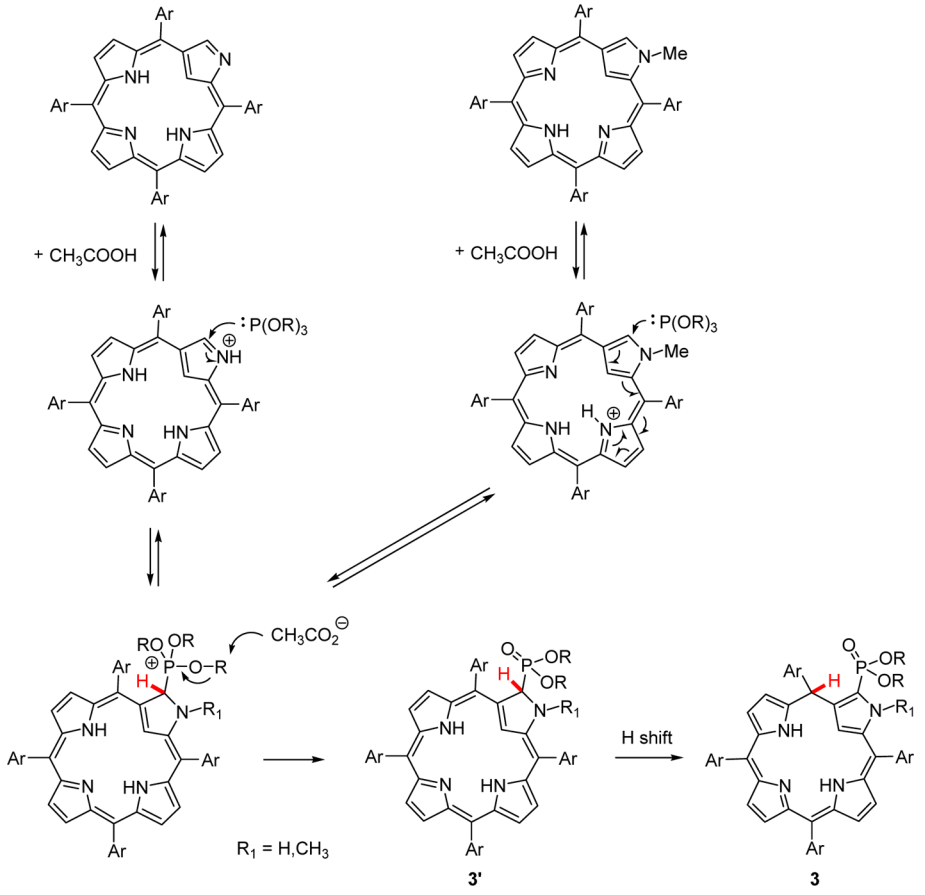

Scheme 3. Synthesis of 3-Phosphorylated NCP

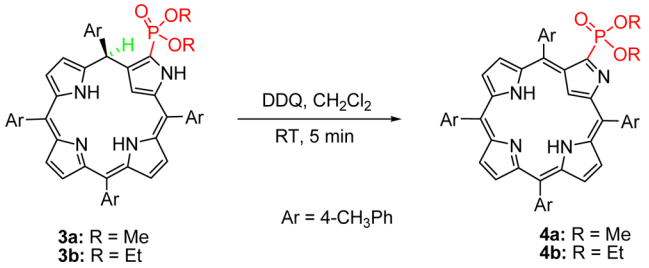

Scheme 4. Insertion of Metal Ions into 4

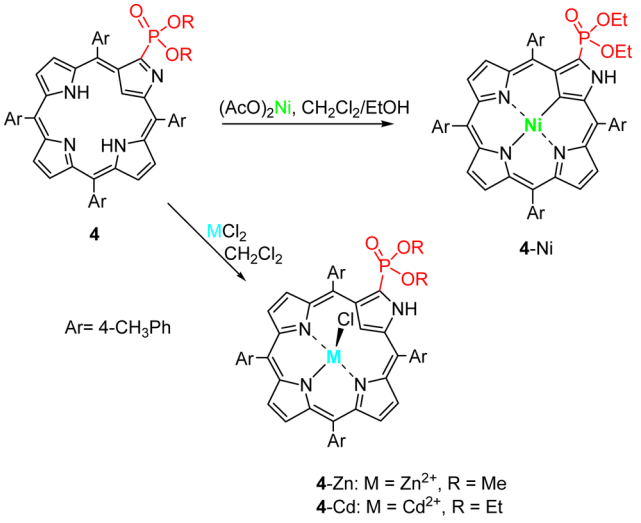

confused pyrrole and P_{21} is 52.5°. The distances of Cd, C21, N2, and C3 atoms from the mean plane are +0.95, −0.26, +1.44, and +1.43 Å, respectively. The mean displacement of the atoms defining P_{21} is 0.21 Å. The β-pyrrole carbons C7, C8, C17, and C18 lie 0.43−0.5 Å under the plane, while C12, C13 lie about 0.3 Å over P_{21}. Because of the nonplanarity, the molecule is chiral, but as it was in the case of crystals of **3b**, crystallization in a centrosymmetric space group *C*2/*c* indicates racemic character of the **4**−Cd crystal phase. The crystal unit cell consists of four pairs of the symmetry-related enantiomers. Within the unit cell the crystal network is organized by many weak interactions of a CH/π H-bond character,[53] but the strongest intermolecular interaction appears to be a double N−H···O═P hydrogen bond involving N2 and O1 of two molecules related by an inversion center (Figure 8). Thus, effectively the crystal lattice is constituted by the heterochiral dimeric assemblies where the enantiomers are held together by forming a ring N2−H2···O1′−P1′−C3′−N2′−H2′···O1−P1− C3 comprising two relatively short intermolecular H-bonds (A···H 1.68 Å, D−A 2.694(5) Å, D−H···A 164.0°). In the case of the zinc complexes of regular 3-dialkylphosphorylporphyrin, formation of dimers was also observed,[42] although they consisted of homochiral subunits linked by coordination of phosphoryl oxygens to the metal centers. On the other hand, likely due to an unfavorable orientation of the P═O moiety, no intermolecular interactions involving the phosphoryl group are observed in the crystal structure of phlorin **3b**, despite the presence of the hydrogen on N2 that could potentially form an analogous H-bond bridge to that observed in the crystal of **4**−Cd.

dx.doi.org/10.1021/jo302689d | *J. Org. Chem.* 2013, 78, 1354−1364

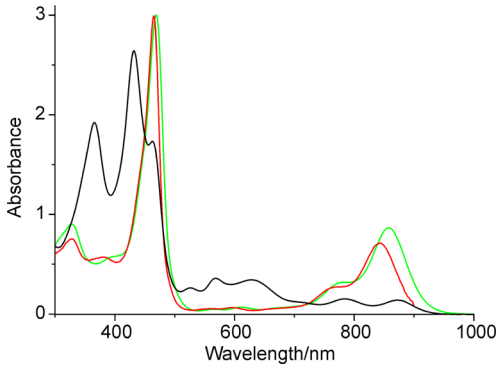

Figure 6. Optical spectra of **4**−Ni (black), **4**−Zn (red), and **4**−Cd (green) in dichloromethane.

Separation of the enantiomers of **4**−Cd was achieved by HPLC performed on a chiral stationary phase with dichloromethane/ethyl acetate as the mobile phase. Despite the expected lability that could result in demetalation on the chromatographic column, the complex turned out to be stable. As it was for the phlorin **3a**, in the case of **4**−Cd the bands consisting of enantiomers overlapped, and thus separation of the slower migrating stereoisomer was incomplete, though the faster band contained pure enantiomer 1 (Figure 9). The optical activity of the fraction was confirmed by the CD spectra showing the most intense Cotton effect near 470 nm, that is at the wavelength of the Soret band in the UV−vis spectrum of **4**−Cd (Figure 9).

The absolute configuration of stereoisomers of **4**−Cd was assigned on the basis of a theoretically predicted CD spectrum of the *S* enantiomer. The sign of the Cotton effect at 470 nm observed for the slower migrating enantiomer **2** is the same as that of the calculated CD spectrum; thus, configuration *S* can be assigned to this stereoisomer. An analogous relation between the absolute configuration and CD response has been observed

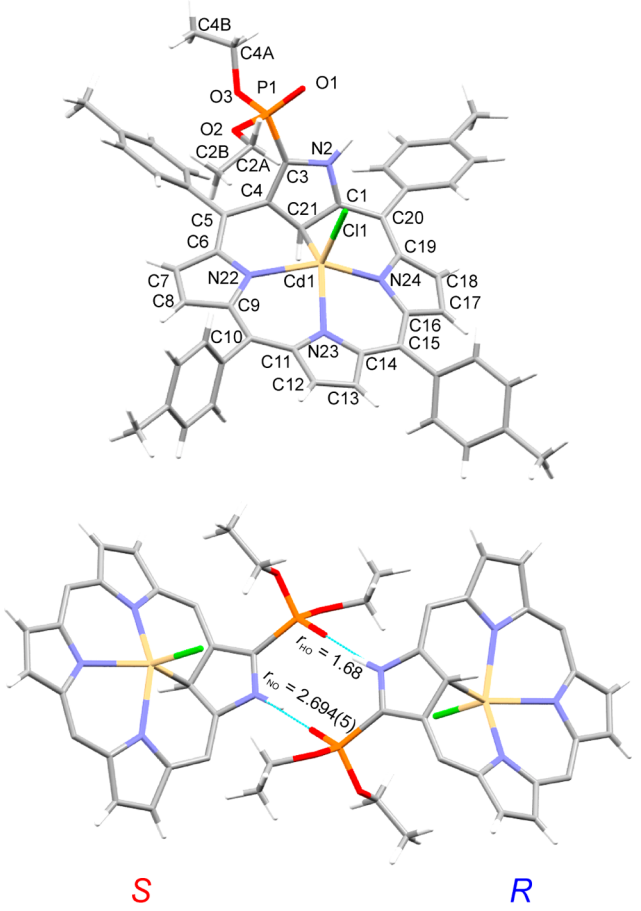

Figure 8. Top: Molecular structure and atom numbering of **4**−Cd (the *S* enantiomer is shown). Bottom: a pair of enantiomers interacting by two hydrogen bonds. The *para*-tolyl substituents in the meso positions of both molecules are omitted for clarity.

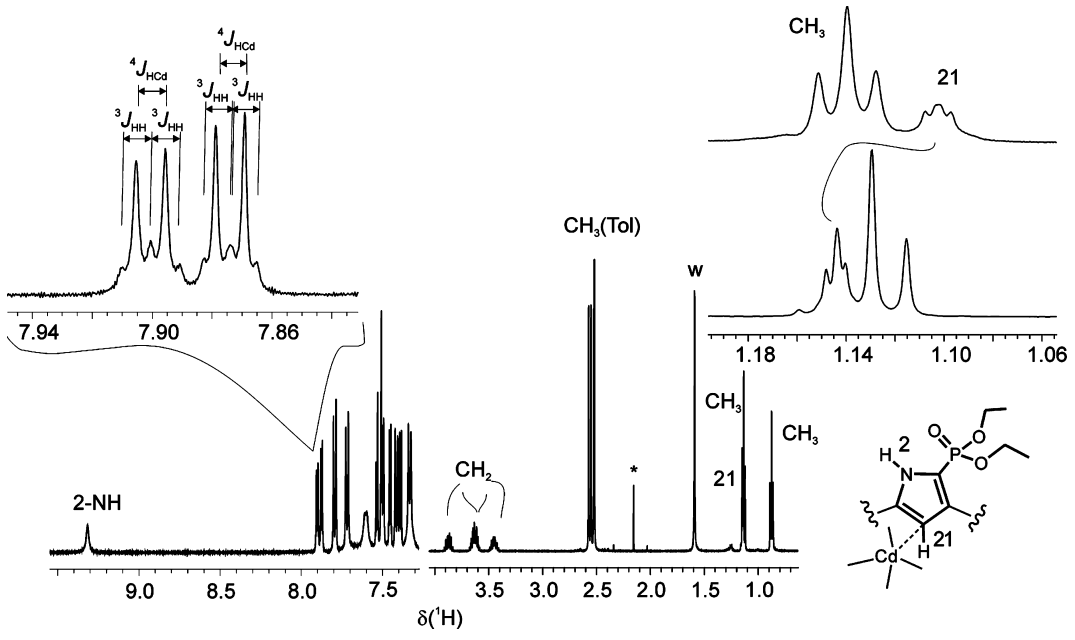

Figure 7. ^{1}H NMR spectrum (600 MHz, $CDCl_3$, 300 K) of **4**−Cd. The inset on the left consists of extension of two *β*-pyrrole signals showing a satellite pattern of scalar coupling with ^{111,113}Cd. The inset on the right presents extension of the region where the signal of 21-CH occurs but which is partially obscured by the signal of one of the methyls at 300 K (lower trace) and can be easily observed at 213 K (higher trace).

dx.doi.org/10.1021/jo302689d | *J. Org. Chem.* 2013, 78, 1354−1364

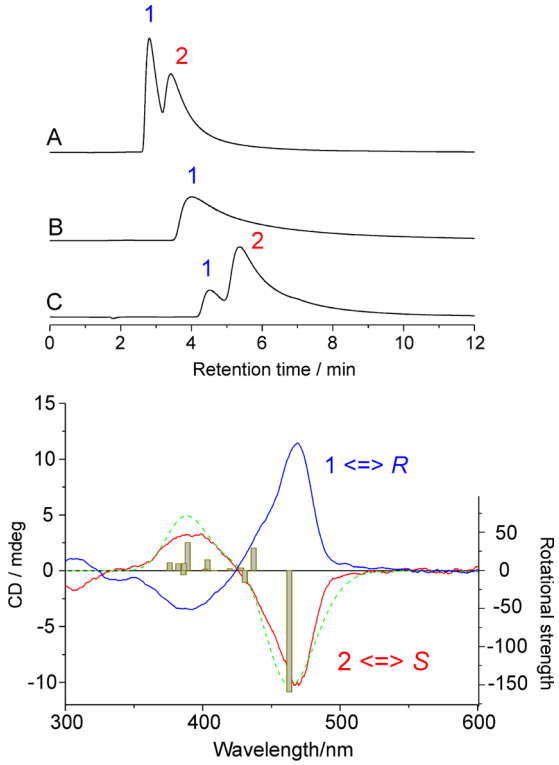

Figure 9. Top: Chiral-phase HPLC profiles (0.5 mg of solute, eluent dichloromethane/ethyl acetate 50/50, flow 2 mL/min, detection at λ = 520 nm) of the racemic **4**−Cd (A) and separated fractions 1 (B) and 2 (C). Bottom: CD spectra of the separated fractions (dichloromethane solutions). The gray bars represent electronic transitions calculated for the enantiomer *S* and the calculated CD spectrum for this enantiomer is drawn as a green dashed line.

recently for other derivatives comprising a chirality plane, such as 21-alkylated or 21-alkoxylated NCP.[48] Our attempt to crystallize the separated enantiomers for both fractions resulted in racemic phases which were isostructural with that already obtained when started from the racemic **4**−Cd. For both enantiomers about 50% decay of the Cotton effect intensities was observed in the CD spectra after 20 h at room temperature, while the UV−vis spectra remained unaltered. These observations indicate slow racemization of **4**−Cd, which is possible due to a labile character of this type of complexes,[59] allowing configuration changes that may result in racemization or enantiomerization in the presence of a chiral anionic ligand.

Dimerization of **4**−Cd in the solid state prompted us to analyze whether an analogous dimer could also be detected in solution. However, in the ^{1}H NMR spectra we did not observe any features indicative for the closeness of the porphyrin molecules, such as up/downfiled shift of certain signals or spectral pattern alteration upon up to 80-fold dilution (10.0−0.12 mM) of the **4**−Cd complex solutions in C_6D_6 or in $CDCl_3$. It may indicate monomeric rather than dimeric character of the complex in solution since upon the concentration change a monomer/dimer equilibrium would cause changes in the chemical shifts of the signals of some protons localized in the vicinity of the bridging moieties.[24] As the dimeric assembly in the solid state consists of heterochiral units, one can expect differences in the spectral properties of the separated enantiomers and the racemic mixture if such a dimer would exist in the solution. Apparently, both ^{1}H NMR and optical spectra of enantiomerically pure and racemic solutions are identical indicating the lack of that kind of dimerization.

CONCLUSION

We have shown that position 3 of NCP can be activated by a weak acid toward reaction with phosphorus-containing nucleophiles under very mild conditions. The reaction of NCP with trialkylphosphites is regiospecific as the substitution by dialkylphosphoryl occurred solely at position 3 but also because the hydrogen is attached in only one site, i.e., *meso*-position 5. The formed phlorins **3** are chiral and relatively stable but can be easily converted to the appropriate achiral porphyrins. Thus, the reaction with phosphites is also a facile method of phosphorylation of NCP. The phosphonate-bearing phlorins or porphyrins as well as their metal complexes can interact with other molecules by means of the $-PO(OR)_2$ group and/or macrocyclic core and thus can form supramolecular complexes and that ability can be potentially applied in chiral recognition. Relations between absolute configurations and CD response established for **3** and **4**−Cd can be also useful in the analysis of stereocontrolled processes of coordination or supramolecular assembling of other structurally related systems. This will be the subject of our further study.

EXPERIMENTAL SECTION

General Methods. All of the reagents from commercial suppliers were used without further purification. All of the solvents were freshly distilled from the appropriate drying agents before use. The analytical TLC was performed with silica gel 60 F254 plates. Column chromatography was carried out by using silica gel 60 (200−300 mesh). The NMR spectra were recorded on a spectrometer operating at 500 or 600 MHz for ^{1}H, 125.6 or 150 MHz for ^{13}C, and 202.4 or 243 MHz for ^{31}P. TMS was used as an internal reference for ^{1}H and ^{13}C chemical shifts and $CDCl_3$ was the solvent. ^{31}P signals were measured in presence of an inset containing 85% H_3PO_4 as the external reference. Mass spectra were recorded using matrix-assisted laser desorption ionization-time-of-flight (MALDI-TOF) or electrospray ionization-time-of-flight (ESI-TOF) methods and calibrated by means of internal standards. 2D experiments were performed using standard pulse sequences. The low-temperature NOESY spectra were recorded with 2048 × 512 data blocks and with a 400 ms mixing time. Resolution of stereoisomers was performed at room temperature on a Chirex 3010 analytical column (25 cm length, 4.6 mm i.d.) packed with 5 μm silica gel coated with covalently bound (*S*)-valine and dinitroaniline. The HPLC-grade solvents were applied.

Calculations. Density functional theory (DFT and TD-DFT) calculations were performed using Gaussian 09.[60] DFT geometry optimizations were carried out in unconstrained C_1 symmetry, using refined X-ray coordinates as starting geometries. DFT geometries were refined to meet standard convergence criteria, and the existence of a local minimum was verified by a normal-mode frequency calculation. DFT calculations were performed using the hybrid functional B3LYP,[61−63] combined with the 6-31G(d,p) and LANL2DZ[64−66] basis sets (**3b** and **4**−Cd, respectively). The electronic and CD spectra were simulated by means of time-dependent density functional theory (TD-DFT). In each case 15 states were calculated. For these calculations, the polarizable continuum model of solvation was used (PCM, dichloromethane), and, in the case of **4**−Cd, the basis set was expanded to 6-311G(d,p). The electronic transitions, UV/vis, and CD spectra were analyzed by means of the GaussSum program.[67] The transitions were convoluted by Gaussian curves with 2000 cm^{-1} and 0.25 eV half line widths for the UV/vis and CD spectra, respectively.

Syntheses of Precursors. Starting porphyrins **1a** and **1b** were synthesized as previously described.[68,69]

3-(Dialkoxyphosphoryl)-5*H*-5,10.15.20-tetrakis(*p*-tolyl)-2-aza-21-carbaphlorins 3. In a typical synthesis of **3**, a solution containing 67 mg (0.1 mmol) of NCP (**1**) and 60 mg (0.5 mmol) of trimethyl phosphite or 80 mg (0.5 mmol) of triethylphosphite and 30 mg (0.5 mmol) of acetic acid in 25 mL of anhydrous and deareated benzene was stirred and heated to reflux for 1.5 h under nitrogen. After that time, TLC showed no NCP reactant left. The solvent was then evaporated, and

dx.doi.org/10.1021/jo302689d | J. Org. Chem. 2013, 78, 1354−1364

the residue was chromatographed on a silica gel column with dichloromethane/methanol mixture (v/v = 100:3) as an eluent. The blue-green colored product fractions were combined together, followed by removal of solvent to afford derivative **3** as a blue powder. Yields: 62 mg (79%) for **3a**, 57 mg (70%) for **3b**, 57 mg (70%) for **3c**.

Selected data for **3a**: ^{1}H NMR (500 MHz, $CDCl_3$, 298 K) δ_H = 2.22 (s, 3H, $-CH_3$), 2.41 (s, 6H, $-CH_3$), 2.43 (s, 3H, $-CH_3$), 3.78 (d, $^3J_{HP}$ = 7.0 Hz, 3H, $-OCH_3$), 3.81 (d, $^3J_{HP}$ = 7.0 Hz, 3H, $-OCH_3$), 5.37 (dd, ^4J = 2.5 Hz, $^4J_{HP}$ = 4.3 Hz 1H, 21-CH), 6.28 (s, 1H, 5-CH), 6.52 (d, J = 4.5 Hz, 1H, pyrrH), 6.57−6.59 (m, 2H, pyrrH), 6.73 (d, J = 5.5 Hz, 1H, pyrrH), 6.84 (d, J = 4.5 Hz, 1H, pyrrH), 6.89 (d, J = 8.0 Hz, 1H, ArH), 6.92 (d, J = 5.5 Hz, 1H, pyrrH), 6.97 (d, J = 8.0 Hz, 2H, ArH), 7.19−7.22 (m, 8H, ArH), 7.30−7. 33(m, 3H, ArH), 8.32 (br, 1H, 24-NH), 8.79 (br, 1H, 22-NH), 8.85 (br, 1H, 2-NH); ^{1}H NMR (500 MHz, $CDCl_3$, 235 K) δ 2.27 (s, 3H, $-CH_3$), 2.45 (s, 6H, $-CH_3$), 2.48 (s, 3H, $-CH_3$), 3.31 (d, J = 11.5 Hz, 3H, $-OCH_3$), 3.93 (d, J = 11.5 Hz, 3H, -OCH_3), 5.29 (s, 1H, 21-CH), 6.29 (s, 1H, 5-CH), 7.24−7.34 (m, 8H, ArH),7.38−7.43 (m, 3H, ArH), 7.72 (d, J = 7.5 Hz, 1H, ArH), 8.24 (br, 1H, 24-NH), 8.75 (br, 1H, 22-NH), 9.06 (br, 1H, 2-NH);^{13}C NMR (125 MHz, $CDCl_3$, 298 K) δ_C = 20.9, 21.3, 21.4, 41.7, 52.9 (d, J_{CP} = 8.1 Hz), 53.1 (d, J_{CP} = 8.1 Hz), 104.9 (d, J_{PC} = 14.3 Hz), 109.3, 112.5, 111.6, 112.7 (d, J_{CP} = 225.6 Hz), 122.8, 127.3, 127.7, 128.0, 128.3, 128.6, 129.0, 129.2, 129.6, 131.0 (d, J_{CP} = 15.7 Hz), 131.2, 132.1, 133.6, 133.8, 134.9, 135.5, 136.18, 136.5, 137.0 (d, J_{CP} = 12.4 Hz), 137.17, 137.19, 137.80, 137.84, 138.0, 139.5, 143.1, 146.1, 151.2, 166.5; ^{31}P NMR (202.4 MHz, $CDCl_3$, H_3PO_4, 298 K) δ_P = 13.9; UV−vis ($CHCl_3$) λ_{max}/nm (log ε) 415 (3.75), 643 (3.27), 696 (3.46); HRMS (ESI-TOF) 781.3305 (obsd), 781.3302 (calcd for $C_{50}H_{46}N_4O_3P$ [M + H]$^+$), ΔM/M = −0.4 ppm.

Selected data for **3b**: ^{1}H NMR (500 MHz, $CDCl_3$, 298K) δ_H = 1.09 (t, J = 7.5 Hz, 3H, $-CH_3$), 1.38 (t, J = 7.5 Hz, 3H, $-CH_3$), 2.24 (s, 3H, $-CH_3$), 2.43 (s, 6H, $-CH_3$), 2.45 (s, 3H, $-CH_3$), 3.58−3.63 (m, 1H, $-OCH_2$), 3.86−3.90 (m, 1H, $-OCH_2$), 4.14−4.19 (m, 1H, $-OCH_2$), 4.22−4.27 (m, 1H, $-OCH_2$), 5.43 (dd, ^4J = 2.6 Hz, $^4J_{HP}$ = 4.5 Hz 1H, 21-CH), 6.36 (s, 1H, 5-CH), 6.53 (d, J = 4.5 Hz, 1H, pyrrH), 6.59 (d, J = 3.5 Hz, 1H, pyrrH), 6.61 (d, J = 3.5 Hz, 1H, pyrrH), 6.73 (d, J = 5.5 Hz, 1H, pyrrH), 6.85 (d, J = 4.5 Hz, 1H, pyrrH), 7.21−7.24 (m, 7H, ArH), 7.32−7.35(m, 4H, ArH), 8.37 (br, 1H, 24-NH), 8.89 (br, 1H, 22-NH), 8.92 (br, 1H, 2-NH); ^{13}C NMR (125 MHz, $CDCl_3$, 298 K) δ_C = 15.98, 16.04, 16.38, 16.44, 20.9, 21.27, 21.35 41.7, 62.5 (d, J_{CP} = 8.1 Hz), 62.6 (d, J_{CP} = 8.1 Hz), 105.1 (d, J_{CP} = 13.6 Hz), 108.2, 109.2, 111.5, 111.7, 114.4 (d, J_{CP} = 224.3 Hz), 122.8, 127.3, 127.6, 127.9, 128.2, 128.5, 128.9, 129.0, 129.6, 130.3 (d, J_{CP} = 16.3 Hz), 131.2, 132.1, 133.5, 133.7, 135.0, 135.4, 136.1, 136.5, 136.6 (d, J_{CP} = 11.7 Hz), 137.2, 137.8, 137.9, 138.0, 139.7, 143.0, 146.1, 151.1, 166.5; ^{31}P NMR (202.4 MHz, chloroform-*d*, H_3PO_4, 298 K) δ_P = 10.9; UV−vis ($CHCl_3$) λ_{max}/nm (log ε) 417 (3.73), 649 (3.25), 698 (3.44); HRMS (ESI-TOF) 809.3618 (obsd), 809.3615 (calcd for $C_{52}H_{50}N_4O_3P$ [M + H]$^+$), ΔM/M = −0.4 ppm.

Selected data for **3c**: ^{1}H NMR (500 MHz, $CDCl_3$, 298 K) δ_H = 2.24 (s, 3H, $-CH_3$), 2.41 (s, 3H, $-CH_3$), 2.43 (s, 3H, $-CH_3$), 2.45 (s, 3H, $-CH_3$), 3.13 (s, 3H, NCH_3), 3.38 (d, J_{HP} = 11.5 Hz, 3H, $-OCH_3$), 3.67 (d, J_{HP} = 11.5 Hz, 3H, $-OCH_3$), 5.05 (d, J_{HP} = 4.5 Hz, 1H, 21-CH), 6.50 (d, J = 4.5 Hz, 1H, pyrrH), 6.61 (d, J = 3.0 Hz, 1H, pyrrH), 6.67 (d, J = 3.0 Hz, 1H, pyrrH), 6.78 (d, J = 5.0 Hz, 1H, pyrrH), 6.85 (d, J = 4.5 Hz, 1H, pyrrH), 6.93 (d, J = 9.0 Hz, 3H, ArH+5-CH), 6.99 (d, J = 8.0 Hz, 2H, ArH), 7.21−7.24 (m, 10H, ArH), 7.32 (d, J = 7.0 Hz, 2H, ArH), 7.63 (br, 1H, 24-NH), 8.07 (br, 1H, 22-NH), 8.82 (br, 1H, 2-NH); ^{13}C NMR (125 MHz, $CDCl_3$, 298 K) δ_C = 21.0, 21.3, 21.4, 34.7, 41.6, 52.3 (d, J_{CP} = 6.1 Hz), 52.5 (d, J_{CP} = 6.1 Hz), 102.9 (d, J_{CP} = 14.4 Hz), 109.4, 110.5, 112.1, 113.2 (d, J_{CP} = 221.5 Hz), 123.3, 127.2, 127.8, 128.96, 127.98, 128.50, 128.8, 129.6, 130.0, 131.5, 132.1, 133.2, 133.8, 135.4, 135.8, 136.47, 136.55, 136.9, 137.0, 137.1, 137.21, 137.71, 137.79, 137.84, 139.6, 141.0, 144.6, 145.3, 150.7, 166.3; ^{31}P NMR (202.4 MHz, $CDCl_3$, H_3PO_4, 298 K) δ_P = 13.9; UV−vis ($CHCl_3$) λ_{max}/nm (log ε) 418 (3.68), 633 (3.25), 685 (3.44); HRMS (ESI-TOF) m/z = 795.3455 (obsd), 795.3459 (calcd for $C_{51}H_{48}N_4O_3P$ [M + H]$^+$), ΔM/M = 0.5 ppm.

3-(Dialkoxyphosphoryl)-5,10.15.20-tetrakis(*p*-tolyl)-2-aza-21-carbaporphyrins 4. In the typical preparation, to a dichloromethane solution of **3** (40 mg, 0.05 mmol) was added 2,3-dichloro-5,6-dicyano-1,4-benzoquinone (30 mg, 14 mmol), and the mixture was stirred for 5 min. After evaporation of the solvent, the components were separated by the silica gel column with a dichloromethane/methanol mixture (v/v = 100:5) as an eluent. The brown fraction contained **4**, which precipitated as a red-brown powder upon addition of hexane. Yields: 25 mg (65%) for **4a**, 24 mg (60%) for **4b**.

Selected data for **4a**: ^{1}H NMR (500 MHz, $CDCl_3$, 298 K) δ_H = −4.33 (d, $^4J_{HP}$ = 2.3 Hz, 1H, 21-CH), 2.67 (s, 3H, $-CH_3$), 2.68 (s, 6H, $-CH_3$), 2.69 (s, 3H, $-CH_3$), 3.52 (d, $^3J_{HP}$ = 11.0 Hz 6H, $-OCH_3$), 7.54 (t, J = 9.0 Hz, 4H, ArH), 7.61 (d, J = 7.5 Hz, 2H, ArH), 8.03 (d, J = 7.5 Hz, 2H, ArH), 7.97 (d, J = 7.5 Hz, 2H, ArH), 8.02 (d, J = 7.5 Hz, 2H, ArH), 8.25−8.28 (m, 4H, ArH), 8.39−8.44 (m, 4H, pyrrH), 8.75 (d, J = 4.5 Hz, 1H, pyrrH), 8.87 (d, J = 4.5 Hz, 1H, pyrrH); ^{13}C NMR (125 MHz, $CDCl_3$, 298 K) δ_C = 21.5, 21.56, 21.64, 53.3 (d, J_{CP} = 6.8 Hz), 93.2, 116.7, 118.8, 125.2, 126.7, 126.8, 127.86, 127.93, 128.0, 128.8, 130.1, 131.4, 133.1, 133.4, 134.66, 134.72, 135.2, 136.7, 136.8, 137.5, 137.6, 138.3, 138.4, 138.5, 138.59, 138.64, 141.6, 142.7, 146.6, 146.9, 148.3, 157.3, 158.8; ^{31}P NMR (202.4 MHz, $CDCl_3$, H_3PO_4, 298 K) δ_P = 13.6; UV−vis ($CHCl_3$) λ_{max}/nm (log ε) 395 (4.56), 452 (5.13), 554 (3.95), 601 (3.86), 773 (4.16); HRMS (ESI-TOF) m/z = 779.3145 (obsd), 779.3146 (calcd for $C_{50}H_{44}N_4O_3P$ [M + H]$^+$), ΔM/M = 0.1 ppm.

Selected data for **4b**: ^{1}H NMR (500 MHz, $CDCl_3$, 298 K) δ_H = −4.40 (d, $^4J_{HP}$ = 2.3 Hz, 1H, 21-CH), 1.01 (t, J = 7.0 Hz, 6H, $-CH_3$), 2.65 (s, 3H, $-CH_3$), 2.66 (s, 3H, $-CH_3$), 2.67 (s, 6H, $-CH_3$), 3.84 (m, 2H, $-OCH_2-$), 3.94 (m, 2H, $-OCH_2-$), 7.52 (d, J = 7.5 Hz, 2H, ArH), 7.53 (d, J = 7.4 Hz, 2H, ArH), 7.58 (d, J = 7.9 Hz, 2H, ArH), 7.64 (d, J = 7.7 Hz, 2H, ArH), 7.97 (d, J = 7.9 Hz, 2H, ArH), 8.01 (d, J = 7.4 Hz, 2H, ArH), 8.23 (d, J = 7.4 Hz, 2H, ArH), 8.25 (d, J = 7.6 Hz, 2H, ArH), 8.38 (d, J = 5.0 Hz, 1H, pyrrH), 8.41 (d, J = 4.8 Hz, 1H, pyrrH), 8.43 (d, J = 4.6 Hz, 1H, pyrrH), 8.44 (d, J = 4.6 Hz, 1H, pyrrH), 8.73 (d, J = 4.9 Hz, 1H, pyrrH), 8.89 (d, J = 4.9 Hz, 1H, pyrrH); ^{13}C NMR (125 MHz, $CDCl_3$, 298 K) δ_C = 21.49, 21.51, 21.65, 62.7 (d, J_{CP} = 6.5 Hz), 94.1, 116.7, 118.6, 125.2, 126.7, 126.8, 127.8, 127.9, 128.6, 130.0, 131.2, 133.3, 133.5, 134.6, 134.7, 135.1, 136.7, 136.9, 137.5, 137.6, 137.7, 138.1, 138.2, 138.49, 138.52, 138.6, 138.7, 141.4, 142.4, 146.7, 147.0, 157.2, 158.5; ^{31}P NMR (202.4 MHz, $CDCl_3$, H_3PO_4, 298 K) δ_P = 11.7. UV−vis (CH_2Cl_2) λ_{max}/nm (log ε) 261 (4.32), 291 (4.37), 394 (sh), 451 (5.25), 516 (sh), 551 (4.03), 599 (3.89), 707 (3.74), 771 (4.20); HRMS ESI-TOF) m/z = 807.3444 (obsd), 807.3459 (calcd for $C_{52}H_{48}N_4O_3P$ [M + H]$^+$), ΔM/M = 1.8 ppm.

(3-(Diethoxyphosphoryl)-5,10.15.20-tetrakis(*p*-tolyl)-2-aza-21-carbaporphyrinato)nickel(II) (4−Ni). To a deareated solution of **4b** (20 mg, 0.024 mmol) in dichloromethane (10 mL) was added a solution of nickel diacetate tetrahydrate (30 mg, 0.12 mmol) in ethanol (5 mL), and the mixture was heated under reflux for 2 h in the atmosphere of nitrogen. The solvent was then removed, and the solid residue was dissolved in dichloromethane and passed down a short silica gel column with dichloromethane as an eluent. The fastest moving green band was collected, solvent was partially evaporated, and compound **4**−Ni was precipitated by addition of hexane. The olive powder was collected by filtration. Yield: 12 mg (55%).

Selected data for **4**−Ni: mp >300 °C; ^{1}H NMR (600 MHz, CD_2Cl_2, 300 K) δ_H = 1.19 (t, J = 7.1 Hz, 6H, $-CH_3$), 2.51 (s, 6H, $-CH_3$), 2.53 (s, 3H, $-CH_3$), 2.55(s, 3H, $-CH_3$), 3.86 (dq, $^3J_{HP}$ = 7.8 Hz, $^3J_{HH}$ = 7.1 Hz, 4H, $-OCH_2-$), 7.25 (d, J = 8.4 Hz, 2H, ArH), 7.34 (d, J = 8.4 Hz, 2H, ArH), 7.35 (d, $^3J_{HH}$ = 5.1 Hz, 1H, pyrrH), 7.36 (d, J = 8.5 Hz, 2H, ArH), 7.45 (d, $^3J_{HH}$ = 5.1 Hz, 1H, pyrrH), 7.47 (d, J = 7.8 Hz, 2H, ArH), 7.51 (d, $^3J_{HH}$ = 5.1 Hz, 1H, pyrrH), 7.54 (d, J = 8.0 Hz, 2H, ArH), 7.55 (d, J = 8.0 Hz, 2H, ArH), 7.58 (d, J = 8.0 Hz, 2H, ArH), 7.61 (d, $^3J_{HH}$ = 4.8 Hz, 1H, pyrrH), 7.64 (d, $^3J_{HH}$ = 4.8 Hz, 1H, pyrrH), 7.69 (d, J = 8.2 Hz, 2H, ArH), 7.76 (d, $^3J_{HH}$ = 5.1 Hz, 1H, pyrrH), 10.61 (br, 1H, 2-NH); ^{13}C NMR (150 MHz, CD_2Cl_2, 300 K) δ_C = 15.4 (d, J_{CP} = 6.8 Hz, $-CH_3$), 20.62, 20.63, 20.67, 20.71, 62.5 (d, J_{CP} = 5.5 Hz, $-OCH_2-$), 110.8, 116.9, 117.5, 119.3, 124.5, 126.0, 127.49, 127.54, 128.2, 129.0, 129.2, 131.9, 132.1, 132.2, 132.4, 132.5, 133.3, 134.3, 135.9, 136.8, 137.1, 137.2, 138.2, 145.5, 148.0, 150.0, 150.7, 154.6, 155.7, 156.7; ^{31}P NMR (243 MHz, CD_2Cl_2, H_3PO_4, 298 K) δ_P = 6.9; UV−vis (CH_2Cl_2) λ_{max}/nm (log ε) 366 (4.41), 431 (4.51), 462 (4.39), 525 (3.35), 566 (3.75), 627 (3.68), 783 (3.26), 871 (3.26); HRMS (ESI-TOF) m/z = 863.2656 (obsd), 863.2656 (calcd for $C_{52}H_{46}N_4O_3PNi$ [M + H]$^+$), ΔM/M = 0.0 ppm.

dx.doi.org/10.1021/jo302689d | *J. Org. Chem.* 2013, 78, 1354−1364

(3-(Dimethoxyphosphoryl)-5,10,15,20-tetrakis(*p*-tolyl)-2-aza-21-carbaporphyrinato)zinc Chloride (4−Zn). A mixture of **4a** (30 mg, 0.038 mg) and zinc(II) chloride (30 mg, 22 mmol) in CH_2Cl_2 (10 mL) was stirred at room temperature for 40 min. Then the reaction mixture was washed three times with water. The organic layer was dried with anhydrous Na_2SO_4, and the solvent was removed under reduced pressure to give the crude product. The crude product was recrystallized from a mixture of toluene/hexane to afford **4**−Zn in 95% yield (32 mg).

Selected data for **4**−Zn: ^{1}H NMR (500 MHz, $CDCl_3$, 298 K) δ_H = 1.24 (dd, ^4J = 1.8 Hz, $^4J_{HP}$ = 4.0 Hz 1H, 21-CH), 2.53 (s, 6H, $-CH_3$), 2.57 (s, 3H, $-CH_3$), 2.58 (s, 3H, $-CH_3$), 3.11 (d, J = 12.0 Hz, 3H, -OCH_3), 3.35 (d, J = 12.0 Hz, 3H, $-OCH_3$), 7.34 (d, J = 9.0 Hz, 4H, ArH), 7.43 (d, J = 7.5 Hz, 2H, ArH), 7.49−7.54 (m, 6H, ArH), 7.62 (br, 2H, ArH), 7.74 (d, J = 9.0 Hz, 2H, pyrrH), 7.81 (m, 2H, pyrrH), 7.96 (d, J = 5.0 Hz, 1H, pyrrH), 8.10 (d, J = 5.0 Hz, 1H, pyrrH), 9.08 (br, 1H, 2-NH); ^{1}H NMR (500 MHz, $CDCl_3$, 243 K) δ_H = 1.23 (dd, ^4J = 2.1 Hz, $^4J_{HP}$ = 4.0 Hz 1H, 21-CH), 2.56 (s, 6H, $-CH_3$), 2.60 (s, 6H, $-CH_3$), 3.12 (d, J = 11.5 Hz, 3H, $-OCH_3$), 3.68 (d, J = 11.5 Hz, 3H, $-OCH_3$), 7.34−7.41 (m, 4H, ArH), 7.47−7.55 (m, 8H, ArH + pyrrH), 7.56 (d, J = 5.0 Hz, 1H, pyrrH), 7.59 (d, J = 5.0 Hz, 1H, pyrrH), 7.75 (d, J = 7.5 Hz, 2H, ArH), 7.78 (d, J = 7.5 Hz, 2H, ArH),7.84 (d, J = 7.0 Hz, 2H, ArH), 8.01 (d, J = 5.0 Hz, 1H, pyrrH), 8.03 (d, J = 5.0 Hz, 1H, pyrrH), 9.16 (br, 1H, 2-NH); ^{13}C NMR (125 MHz, $CDCl_3$, 298 K) δ_C = 21.4, 21.5, 53.0 (d, J_{CP} = 8.1 Hz), 54.1 (d, J = 8.1 Hz), 72.5 (d, J_{CP} = 11.0 Hz), 107.1 (d, J_{CP} = 215.3 Hz), 117.0, 117.39, 127.6, 128.0, 128.9, 129.3, 132.4, 133.1, 133.3, 133.8, 133.9, 134.0, 134.2, 134.5, 135.28, 135.35, 135.5, 137.1, 137.6, 137.7, 137.9, 138.9, 140.1, 153.1, 158.5, 159.1, 164.7, 165.5; ^{31}P NMR (202.4 MHz, $CDCl_3$, H_3PO_4, 298 K) δ_P = 8.9. UV−vis ($CHCl_3$) λ_{max}/nm (log ε) 327 (4.44), 381 (4.32), 465 (5.02), 759 (4.01), 842 (4.41); HRMS (ESI-TOF) m/z = 841.2272 (obsd), 841.2281 (calcd for $C_{50}H_{42}N_4O_3PZn$ [M − Cl]$^+$), ΔM/M = 1.1 ppm.

(3-(Diethoxyphosphoryl)-5,10,15,20-tetrakis(*p*-tolyl)-2-aza-21-carbaporphyrinato)cadmium Chloride (4−Cd). A mixture of **4b** (30 mg, 0.037 mg) and anhydrous cadmium chloride (30 mg, 16 mmol) in CH_2Cl_2 (10 mL) was stirred at room temperature for 12 h. The reaction mixture was then filtered on a sintered glass microfilter, solvent was evaporated, the solid residue was dissolved in 5 mL of benzene, and the solution was filtered by means of polystyrene microfilter. The complex **4b** formed dark green crystals upon addition of an equal volume of hexane. Yield: 28 mg (80%).

Selected data for **4**−Cd: mp >250 °C dec; ^{1}H NMR (500 MHz, $CDCl_3$, 298 K) δ_H = 0.87 (t, J = 7.0 Hz, 3H, $-CH_3$), 1.13 (t, J = 7.1 Hz, 3H, $-CH_3$), 1.14 (m, 1H, 21-CH), 2.52 (s, 3H, $-CH_3$), 2.52 (s, 3H, $-CH_3$), 2.55 (s, 3H, $-CH_3$), 2.57 (s, 3H, $-CH_3$), 3.45 (m, 1H, $-OCH_2-$), 3.63 (m, 2H, $-OCH_2-$), 3.87 (m, 1H, $-OCH_2-$), 7.33 (d, J = 8.0 Hz, 3H, ArH), 7.39 (d + dd, $^3J_{HH}$ = 4.9 Hz, $^4J_{HCd}$ = 4.0 Hz, 1H, pyrrH), 7.41 (d, J = 7.8 Hz, 2H, ArH), 7.45 (d + dd, $^3J_{HH}$ = 4.7 Hz, $^4J_{HCd}$ = 3.6 Hz, 1H, pyrrH), 7.499 (d, 2H, J = 7.3, ArH), 7.503 (d + dd, $^3J_{HH}$ = 4.9 Hz, $^4J_{HCd}$ = 4.0 Hz, 1H, pyrrH), 7.53 (d + dd, $^3J_{HH}$ = 4.9 Hz, $^4J_{HCd}$ = 4.9 Hz, 1H, pyrrH), 7.60 (br, 2H, ArH), 7.72 (d, J = 7.7 Hz, 2H, ArH), 7.79 (d, J = 8.1 Hz, 2H, ArH), 7.87 (d + dd, $^3J_{HH}$ = 4.8 Hz, $^4J_{HCd}$ = 4.3 Hz, 1H, pyrrH), 7.90 (d + dd, $^3J_{HH}$ = 4.9 Hz, $^4J_{HCd}$ = 4.9 Hz, 1H, pyrrH), 9.32 (br, 1H, 2-NH); ^{13}C NMR (125 MHz, $CDCl_3$, 298 K) δ_C = 15.9 (d, J_{CP} = 7.0 Hz, $-CH_3$), 16.0 (d, J_{CP} = 7.0 Hz, $-CH_3$), 21.4, 21.5, 62.8 (d, J_{CP} = 5.7 Hz, −OCH_2), 64.0 (d, J_{CP} = 3.9 Hz, -OCH_2), 69.8 (d, J_{CP} = 12.5 Hz, C21), 110.2 (d, J_{CP} = 211.5 Hz, C3), 118.1, 118.5, 127.8, 128.0, 129.5, 129.6 (d, J_{CP} = 13.2 Hz), 132.8, 133.3, 133.9, 134.2, 134.3, 134.4, 134.6, 134.7, 134.9, 135.0, 135.3, 135.5, 137.02, 137.05, 137.9, 138.1, 138.3, 138.9, 140.1, 153.5, 153.6, 160.3, 161.9, 165.0, 165.9; ^{31}P NMR (243 MHz, CD_2Cl_2, H_3PO_4, 298 K) δ_P = 5.4. UV−vis (CH_2Cl_2) λ_{max}/nm (log ε) 216 (4.25), 328 (4.47), 3.89 (sh), 469 (4.99), 560 (sh), 611 (3.35), 676 (sh), 777 (sh), 859 (4.45); HRMS (ESI-TOF) m/z = 919.2361 (obsd), 919.2350 (calcd for $C_{52}H_{46}N_4O_3PCd$ [M − Cl]$^+$), ΔM/M = −1.2 ppm, 955.2100 (obsd), 955.2110 (calcd for $C_{52}H_{47}N_4O_3PClCd$ [M + H]$^+$), ΔM/M =1.0 ppm.

Crystallographic Data. The structures were solved by direct methods using the SHELXS program.[70] All non-hydrogen atoms were refined anisotropically by full matrix least-squares with SHELXL-97.[70] All H atoms, including those located in the difference density map, were placed in calculated positions and refined as the riding model with U_{iso}(H) = 1.2U_{eq}(C).

X-ray quality crystals of **3b** were obtained by slow evaporation of chloroform from the solution. Crystal data for **3b**: $C_{52}H_{49}N_4O_3P\cdot CHCl_3$, M_r = 928.29, T = 100(2) K, CuKα radiation, triclinic, space group $P\bar{1}$, a = 9.708(3) Å, b = 15.036(2) Å, c = 16.375(4) Å, α = 91.37 (2)°, β = 97.32(2)°, γ = 91.43(2)°, V = 2368.3(9) Å^3, Z = 2, D_c = 1.302 Mg m^{-3}, λ = 1.54178 Å, μ = 2.449 mm^{-1}, diffractometer with CCD detector, 2.72 ≤ θ ≤ 59.00°, 15769 collected reflections, 6745 independent reflections, 590 parameters, $R_1(F)$ = 0.1156, $wR_2(F^2)$ = 0.3018, S = 1.553, largest difference peak and hole 0.471 and −0.510 e·Å^{-3}. The asymmetric unit consists of one molecule of **3b** and one molecule of chloroform. One of the ethyl substituents is disordered over two equally occupied positions. The low quality of the crystal, which was caused by partial loss of the cocrystallized chloroform solvent, was responsible for the weak diffraction observed for θ > 59°, resulting in relatively low precision of the crystal data and structural parameters. Unfortunately, other attempts to grow X-ray quality crystals were not successful.

X-ray quality crystals of **4**−Cd were obtained by slow diffusion of the benzene solution of **4**−Cd into hexane at room temperature. Crystal data for **4**−Cd: $C_{52}H_{46}CdClN_4O_3P$, M_r = 953.75, T = 100(2) K, MoKα radiation, monoclinic, space group $C2/c$, a = 28.913(1) Å, b = 11.6762(4) Å, c = 31.837 (2) Å, α = 90.00°, β = 104.692(4)°, γ = 90.00°, V = 10396.7(8) Å^3, Z = 8, D_c = 1.219 Mg m^{-3}, λ = 0.71073 Å, μ = 0.544 mm^{-1}, diffractometer with CCD detector, 2.74 ≤ θ ≤ 27.00°, 26730 collected reflections, 11195 independent reflections, 558 parameters, $R_1(F)$ = 0.071, $wR_2(F^2)$ = 0.1612, S = 1.063, largest difference peak and hole 1.301 and −1.107 e·Å^{-3}. One of the ethyl substituents is disordered over two equally occupied positions.

■ ASSOCIATED CONTENT

Ⓢ Supporting Information

Crystallographic data (CIF), calculation details (Table S1), Cartesian coordinates for the optimized structures (Table S2 and S3), calculated electronic transitions (Table S4 and S5), 1D and 2D NMR, and mass spectra. This material is available free of charge via the Internet at http://pubs.acs.org.

■ AUTHOR INFORMATION

Corresponding Author

*E-mail: lixiaofang@iccas.ac.cn, piotr.chmielewski@chem.uni.wroc.pl.

Notes

The authors declare no competing financial interest.

■ ACKNOWLEDGMENTS

This work was supported by the National Natural Science Foundation of China (Grant No. 20971041), the Key Project of Chinese Ministry of Education (Grant No. 210146), the Open Project Program of Key Laboratory of Theoretical Chemistry and Molecular Simulation of Ministry of Education, Hunan University of Science and Technology, and the Polish National Science Center (Grant No. 2012/04A/ST5/00593). Quantum chemical calculations were performed in the Wrocław Center for Networking and Supercomputing.

■ REFERENCES

(1) Furuta, H.; Asano, T.; Ogawa, T. *J. Am. Chem. Soc.* **1994**, *116*, 767−768.

(2) Chmielewski, P. J.; Latos-Grażyński, L.; Rachlewicz, K.; Głowiak, T. *Angew. Chem., Int. Ed. Engl.* **1994**, *33*, 779−781.

(3) Toganoh, M.; Furuta, H. *Chem. Commun.* **2012**, *48*, 937−954.

(4) Niino, T.; Toganoh, M.; Andrioletti, B.; Furuta, H. *Chem. Commun.* **2006**, 4335−4337.

(5) Yamamoto, T.; Toganoh, M.; Furuta, H. *Dalton Trans.* **2012**, *41*, 9154−9157.

(6) Xie, Y.; Morimoto, T.; Furuta, H. *Angew. Chem., Int. Ed.* **2006**, *45*, 6907−6910.
(7) Zilbermann, I.; Meron, E.; Maimon, E.; Soifer, L.; Elbaz, L.; Korin, E.; Bettelheim, A. *J. Porphyrins Phthalocyanines* **2006**, *10*, 63−66.
(8) Maeda, H.; Morimoto, T.; Osuka, A.; Furuta, H. *Chem.—Asian J.* **2006**, *1*, 832−844.
(9) Maeda, H.; Furuta, H. *Pure Appl. Chem.* **2006**, *78*, 29−44.
(10) Hung, C.-H.; Chang, C.-S.; Ching, W.-M.; Chuang, C.-H. *Chem. Commun.* **2006**, 1866−1868.
(11) Toganoh, M.; Miyachi, T.; Akimaru, H.; Ito, F.; Nagamura, T.; Furuta, H. *Org. Biomol. Chem.* **2009**, *7*, 3027−3030.
(12) Toganoh, M.; Ogawa, H.; Morimoto, T.; Furuta, H. *Supramol. Chem.* **2009**, *21*, 324−330.
(13) Poon, C.-T.; Zhao, S.; Wong, W. K.; Kwong, D. J. *Tetrahedron Lett.* **2010**, *51*, 664−668.
(14) D'Souza, F.; Smith, P. M.; Rogers, L.; Zandler, M. E.; Islam, D.-M. S.; Araki, Y.; Ito, O. *Inorg. Chem.* **2006**, *45*, 5057.
(15) Thomas, A. P.; Babu, P. S. S.; Nair, S. A.; Ramakrishnan, S.; Ramaiah, D.; Chandrashekar, T. K.; Srinivasan, A.; Pillai, M. R. *J. Med. Chem.* **2012**, *55*, 5110−5120.
(16) Du, Y.; Zhang, D.; Chen, W.; Zhang, M.; Zhou, Y.; Zhou, X. *Bioorg. Med. Chem.* **2010**, *18*, 1111−1116.
(17) Ikawa, Y.; Harada, H.; Toganoh, M.; Furuta, H. *Bioorg. Med. Chem. Lett.* **2009**, *19*, 2448−2452.
(18) Ikawa., Y.; Moriyama, S.; Harada, H.; Furuta, H. *Org. Biomol. Chem.* **2008**, *6*, 4157−4166.
(19) Chmielewski, P. J. *Org. Lett.* **2005**, *7*, 1789−1792.
(20) Furuta, H.; Ishizuka, T.; Osuka, A.; Dejima, H.; Nakagawa, H.; Ishikawa, Y. *J. Am. Chem. Soc.* **2001**, *123*, 6207−6208.
(21) Furuta, H.; Ishizuka, T.; Osuka, A.; Ogawa, T. *J. Am. Chem. Soc.* **2000**, *122*, 5748.
(22) Qu, W.; Ding, T.; Cetin, A.; Harvey, J. D.; Taschner, M. J.; Ziegler, C. J. *J. Org. Chem.* **2006**, *71*, 811−814.
(23) Xiao, Z.; Patrick, B. O.; Dolphin, D. *Chem. Commun.* **2002**, 1816−1817.
(24) Chmielewski, P. J.; Maciołek, J.; Szterenberg, L. *Eur. J. Org. Chem.* **2009**, 3930−3939.
(25) Li, X.; Liu, B.; Yi, P.; Yi, R.; Yu, X.; Chmielewski, P. J. *J. Org. Chem.* **2011**, *76*, 2345−2349.
(26) Ishizuka, T.; Yamasaki, H.; Osuka, A.; Furuta, H. *Tetrahedron* **2007**, *63*, 5137−5147.
(27) Jiang, H.-W.; Hao, F.; Chen, Q.-Y.; Xiao, J.-C.; Liu, S. B.; Gu, Y.-C. *J. Org. Chem.* **2010**, *75*, 3511−3514.
(28) Chmielewski, P. J. *Inorg. Chem.* **2007**, *46*, 1617−1626.
(29) Xiao, Z.; Patrick, B. O.; Dolphin, D. *Chem. Commun.* **2003**, 1062−1063.
(30) Xiao, Z.; Patrick, B. O.; Dolphin, D. *Inorg. Chem.* **2003**, *42*, 8125−8127.
(31) Hao, F.; Jiang, H.-W.; Zong, G.; Zhou, Z.; Du, R.-B.; Chen, Q.-Y.; Xiao, J. C. *J. Org. Chem.* **2012**, *77*, 3604−3608.
(32) Toganoh, M.; Kimura, T.; Furuta, H. *Chem. Commun.* **2008**, 102−104.
(33) Toganoh, M.; Kimura, T.; Furuta, H. *Chem.—Eur. J.* **2008**, *14*, 10585−10594.
(34) Jiang, H.-W.; Chen, Q.-Y.; Xiao, J.-C.; Gu, Y.-C. *Chem. Commun.* **2009**, 3732−3734.
(35) Grzegorzek, N.; Pawlicki, M.; Latos-Grażyński, L. *J. Org. Chem.* **2009**, *74*, 8547−8553.
(36) Li, X.; Chmielewski, P. J.; Xiang, J.; Xu, J.; Jiang, L.; Li, Y.; Liu, H.; Zhu, D. *J. Org. Chem.* **2006**, *71*, 9739−9742.
(37) Haase, M.; Goerls, H.; Anders, E. *Synthesis* **1998**, 195−200.
(38) Haase, M.; Gunther, W.; Gorls, H.; Anders, E. *Synthesis* **1999**, 2071−2081.
(39) Akiba, K.-Y.; Negishi, Y.; Kurumaya, K.; Ueyama, N.; Inamoto, N. *Tetrahedron Lett.* **1981**, *22*, 4977−4980.
(40) Grzegorzek, N.; Latos-Grażyński, L.; Szterenberg, L. *Org. Biomol. Chem.* **2012**, *10*, 8064−8075.
(41) Grzegorzek, N.; Pawlicki, M.; Szterenberg, L.; Latos-Grażyński, L. *J. Am. Chem. Soc.* **2009**, *131*, 7224−7225.
(42) Vinogradova, E. V.; Enakieva, Y. Y.; Nefedov, S. E.; Birin, K. P.; Tsivadze, A. Y.; Gorbunova, Y. G.; Bessmertnykh Lemeune, A. G.; Stern, C.; Guilard, R. *Chem.—Eur. J.* **2012**, *18*, 15092−15104.
(43) Atefi, F.; McMurtrie, J. C.; Turner, P.; Duriska, M.; Arnold, D. P. *Inorg. Chem.* **2006**, *45*, 6479−6489.
(44) Matano, Y.; Matsumoto, K.; Terasaka, Y.; Hotta, H.; Araki, Y.; Ito, O.; Shiro, M.; Sasamori, T.; Tokitoh, N.; Imahori, H. *Chem.—Eur. J.* **2007**, *13*, 891−901.
(45) Matano, Y.; Marsumoto, K.; Nakao, Y.; Uno, H.; Sakaki., S.; Imahor, H. *J. Am. Chem. Soc.* **2008**, *130*, 4588−4589.
(46) Enakieva, Y.; Bessmertnykh, A. G.; Gorbunova, Y. G.; Stern, C.; Rousselin, Y.; Tsivadze, A. Y.; Guilard, R. *Org. Lett.* **2009**, *11*, 3842−3845.
(47) Atefi, F.; McMurtrie, J. C.; Arnold, D. P. *Dalton Trans.* **2007**, 2163−2170.
(48) Chmielewski, P. J.; Szterenberg, L.; Siczek, M. *Chem.—Eur. J.* **2011**, *17*, 1009−1020.
(49) Chmielewski, M. J.; Pawlicki, M.; Sprutta, N.; Szterenberg, L.; Latos-Grażyński, L. *Inorg. Chem.* **2006**, *45*, 8664−8671.
(50) LeSaulnier, T. D.; Graham, B. W.; Geier, G. R., III. *Tetrahedron Lett.* **2005**, *46*, 5633−5637.
(51) Pistner, A. J.; Yap, G. P. A.; Rosenthal, J. *J. Phys. Chem.C* **2012**, *116*, 16918−16924.
(52) O'Brien, A. Y.; McGann, J. P.; Geier, G. R., III. *J. Org. Chem.* **2007**, *72*, 4084−4092.
(53) Nishio, M. *Cryst. Eng. Comm.* **2004**, *6*, 130−138.
(54) Furuta, H.; Ishizuka, T.; Osuka, A. *J. Am. Chem. Soc.* **2002**, *124*, 5622−5623.
(55) Furuta, H.; Morimoto, T.; Osuka, A. *Inorg. Chem.* **2004**, *43*, 1618−1624.
(56) Jakobsen, H. J.; Ellis, P. D.; Inners, R. R.; Jensen, C. F. *J. Am. Chem. Soc.* **1982**, *104*, 7742.
(57) Stępień, M.; Latos-Grażyński, L. *J. Am. Chem. Soc.* **2002**, *124*, 3838−3839.
(58) Stępień, M.; Latos-Grażyński, L.; Szterenberg, L.; Panek, J.; Latajka, Z. *J. Am. Chem. Soc.* **2004**, *126*, 4566−4580.
(59) Toganoh, M.; Harada, N.; Morimoto, T.; Furuta, H. *Chem.—Eur. J.* **2007**, *13*, 2257−2265.
(60) Gaussian 09, Revision B.01: Frisch, M. J.; Trucks, G. W.; Schlegel, H. B.; Scuseria, G. E.; Robb, M. A.; Cheeseman, J. R.; Scalmani, G.; Barone, V.; Mennucci, B.; Petersson, G. A.; Nakatsuji, H.; Caricato, M.; Li, X.; Hratchian, H. P.; Izmaylov, A. F.; Bloino, J.; Zheng, G.; Sonnenberg, J. L.; Hada, M.; Ehara, M.; Toyota, K.; Fukuda, R.; Hasegawa, J.; Ishida, M.; Nakajima, T.; Honda, Y.; Kitao, O.; Nakai, H.; Vreven, T. Montgomery, J. A., Jr.; Peralta, J. E.; Ogliaro, F.; Bearpark, M.; Heyd, J. J.; Brothers, E.; Kudin, K. N.; Staroverov, V. N.; Keith, T.; Kobayashi, R.; Normand, J.; Raghavachari, K.; Rendell, A.; Burant, J. C.; Iyengar, S. S.; Tomasi, J.; Cossi, M.; Rega, N.; Millam, J. M.; Klene, M.; Knox, J. E.; Cross, J. B.; Bakken, V.; Adamo, C.; Jaramillo, J.; Gomperts, R.; Stratmann, R. E.; Yazyev, O.; Austin, A. J.; Cammi, R.; Pomelli, C.; Ochterski, J. W.; Martin, R. L.; Morokuma, K.; Zakrzewski, V. G.; Voth, G. A.; Salvador, P.; Dannenberg, J. J.; Dapprich, S.; Daniels, A. D.; Farkas, O.; Foresman, J. B.; Ortiz, J. V.; Cioslowski, J.; Fox, D. J. Gaussian, Inc., Wallingford, CT, 2010.
(61) Becke, A. D. *Phys. Rev. A* **1988**, *38*, 3098−3100.
(62) Becke, A. D. *J. Chem. Phys.* **1993**, *98*, 5648.
(63) Lee, C.; Yang, W.; Parr, R. G. *Phys. Rev. B* **1988**, *37*, 785−789.
(64) Hay, P. J.; Wadt, W. R. *J. Chem. Phys.* **1985**, *82*, 270−283.
(65) Wadt, W. R.; Hay, P. J. *J. Chem. Phys.* **1985**, *82*, 284−298.
(66) Hay, P. J.; Wadt, W. R. *J. Chem. Phys.* **1985**, *82*, 299−310.
(67) O'Boyle, N. M.; Tenderholt, A. L.; Langner, K. M. *J. Comput. Chem.* **2008**, *29*, 839−845.
(68) Geier, G. R., III; Haynes, D. M.; Lindsey, J. S. *Org. Lett.* **1999**, *1*, 1455−1458.
(69) Chmielewski, P. J.; Latos-Grażyński, L. *J. Chem. Soc., Perkin Trans. 2* **1995**, 503−509.
(70) Sheldrick, G. M. *Acta Crystallogr.* **2008**, *A64*, 112−122.